Optical Materials xxx (2015) xxx–xxx

Contents lists available at ScienceDirect

Optical Materials

journal homepage: www.elsevier.com/locate/optmat

Specific features of the electronic structure and optical properties of skutterudites $LaFe_4X_{12}$ (X = P, As and Sb)

A.H. Reshak [a,b,*]

[a] New Technologies – Research Centre, University of West Bohemia, Univerzitni 8, 306 14 Pilsen, Czech Republic
[b] Center of Excellence Geopolymer and Green Technology, School of Material Engineering, University Malaysia Perlis, 01007 Kangar, Perlis, Malaysia

ARTICLE INFO

Article history:
Received 1 May 2015
Received in revised form 27 May 2015
Accepted 8 June 2015
Available online xxxx

Keywords:
Filled skutterudite
Electronic band structure
Fermi surface
Electronic charge density distribution
Optical properties

ABSTRACT

We have reported comprehensive calculation for electronic band structure, density of states, Fermi surface and the optical properties of $LaFe_4X_{12}$ (X = P, As and Sb) compounds. The experimental lattice constant a and the two internal free parameters u and v were optimized by minimizing the total energy using the full potential linear augmented plane wave (*FPLAPW + lo*) method within the local density approximation (*LDA*). The experimental atomic positions were optimized using the *FPLAPW + lo* method within Perdew, Burke and Ernzerhof generalized gradient approximation (*PBE-GGA*). From the obtained relaxed geometry the electronic band structure, the chemical bonding, electronic charge density and the optical properties have been determined using *FPLAPW + lo* within the recently modified Becke–Johnson potential (*mBJ*). It has been found that substituting P → As → Sb show significant influence on the bands/states dispersions. The calculated values of the density of the states at Fermi level $N(E_F)$ and the associated electronic specific heat coefficient (γ) are increases with substituting P → As → Sb that is attributed to the fact that below Fermi level (E_F) there exists several bands with less dispersion moves close to E_F when we substitute P → As → Sb. The bonds nature and the interactions between the atoms were investigated in two crystallographic planes namely (100) and (101). The Fermi surface is formed by two bands which are mainly consist of Fe-d states and X-p states. The observed Fermi surface consists of empty areas that represent the holes and shaded areas corresponding to the electrons. The calculated optical properties exhibit that there exists two lossless regions also it shows that the spectral structure shift toward lower energies when we replace P by As and As by Sb.

© 2015 Elsevier B.V. All rights reserved.

1. Introduction

The filled skutterudite compounds have attracted much attention as a potential candidates for electrical and magnetic application. The filled skutterudite compounds are promising materials for thermoelectric applications [1] due to their high carrier mobility, low lattice thermal conductivity and low electrical resistivity [1–3]. Several interesting phenomena have been observed in these materials, for instance semiconductivity [4,5], superconductivity [6–8], magnetic order [9–13], metal–insulator transition material [14], and valence fluctuation and heavy fermion behavior [15–17]. Among the filled skutterudite compounds are the La-based filled skutterudite phosphide, arsenide and antimonide [18,19]. Harima and Takegahara [20] have calculated the band structure and Fermi surface of $LaFe_4X_{12}$ (X = P, As and Sb) compounds. Takegahara and Harima [21] have used the full potential linear augmented plane wave (*FPLAPW*) method within the local density approximation (*LDA*) to investigate the band structure of simple cubic $LaRu_4P_{12}$ and the orthorhombic $LaFe_4P_{12}$ compounds. Further, they have investigated the Fermi surface and the hybridization between La-f orbital and P-p states. Hachemaoui et al. [22] report an *ab initio* calculation using *LDA* to investigate the structural and elastic properties of $LaFe_4X_{12}$ (X = P, As and Sb) compounds. Nouneh et al. [23] have performed complex band structure calculations for $LaFe_4Sb_{12}$ and $CeFe_4Sb_{12}$ compounds using tight-binding linear muffin-tin orbital (*TB-LMTO*) and full potential linear augmented plane wave (*FPLAPW*) methods to calculate the density of states near Fermi level and the corresponding thermoelectric properties. Nouneh et al. [24] have measured the photoinduced second harmonic generation of $LaFe_4Sb_{12}$ near spin fluctuated critical points. We would like to mentioned that the

* Address: New Technologies – Research Centre, University of West Bohemia, Univerzitni 8, 306 14 Pilsen, Czech Republic.
E-mail address: maalidph@yahoo.co.uk

http://dx.doi.org/10.1016/j.optmat.2015.06.019
0925-3467/© 2015 Elsevier B.V. All rights reserved.

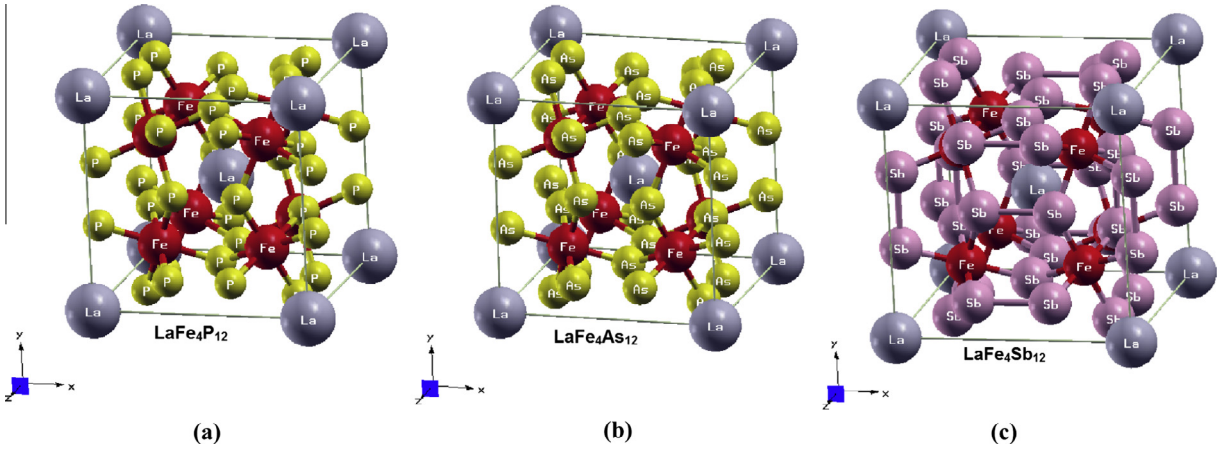

Fig. 1. Calculated crystal structure of $LaFe_4X_{12}$ (X = P, As and Sb) compounds.

Table 1
The calculated lattice constant, the free internal parameters u and v and the bulk modulus B in (GPa) and its pressure derivative, B' in comparison with the experimental data and the previous theoretical results.

$LaFe_4P_{12}$	$LaFe_4As_{12}$	$LaFe_4Sb_{12}$
a (Å)		
7.8315*	8.3251*	9.1392*
7.724[a]	8.179[a]	8.963[a]
7.8316[b] (Exp.)	8.3252[c] (Exp.)	9.1392[d] (Exp.)
7.8217[f]	8.3252[f]	9.1487[e] (Exp.)
		9.1395[f]
u		
0.3530*	0.3453*	0.3365*
0.3527[a]	0.3418[a]	0.3344[a]
0.3539[b] (Exp.)	0.34556[c](Exp.)	0.33696[d] (Exp.)
v		
0.1511*	0.15521*	0.1610*
0.1543[a]	0.15667[a]	0.1612[a]
0.1504[b] (Exp.)	0.15474[c] (Exp.)	0.16042[d] (Exp.)
B		
160.2*	145.7*	104.5*
177.11[a]	152.09[a]	115.82[a]
		88.9[e] (Exp.)
		101.4[e] (calc.)
B'		
3.60*	3.1*	2.98*
4.21[a]	4.03[a]	3.49[a]

[a] Ref. [22].
[b] Ref. [19].
[c] Ref. [36].
[d] Ref. [37].
[e] Ref. [38].
[f] Ref. [20].
* This work.

contribution of the phonon subsystem and the sixteen spin configurations of Fe play a principal role in these compounds [25,26].

From above it is clear that there exist a number of band structure calculations for $LaFe_4X_{12}$ (X = P, As and Sb) compounds using different methods within local density approximation (*LDA*) and generalized gradient approximation (*GGA*) as exchange- correlation potentials. It is well know that for the highly correlated compounds, *LDA* and *GGA* are known to fail to give the correct ground state. In these systems, the electrons are highly localized. The Coulomb repulsion between the electrons in open shells should be taken into account [27]. Therefore, this motivates us to address ourselves for a comprehensive theoretical calculation using the all-electron full potential linear augmented plane wave plus the local orbitals (*FPLAPW + lo*) method within the recently modified Becke–Johnson potential (*mBJ*) [28], which optimizes the corresponding potential for electronic band structure calculations. The modified Becke–Johnson potential allows the calculation with accuracy similar to the very expensive GW calculations [28]. It is a local approximation to an atomic "exact-exchange" potential and a screening term. We have calculated the electronic band structure, electronic charge distribution, total and the angular momentum resolved projected density of states, Fermi surface and the optical properties for $LaFe_4X_{12}$ (X = P, As and Sb) compounds. The investigation of the optical properties brings deep insight to understand the origin of the electronic band structure. Therefore, we are interested to calculate the optical properties of

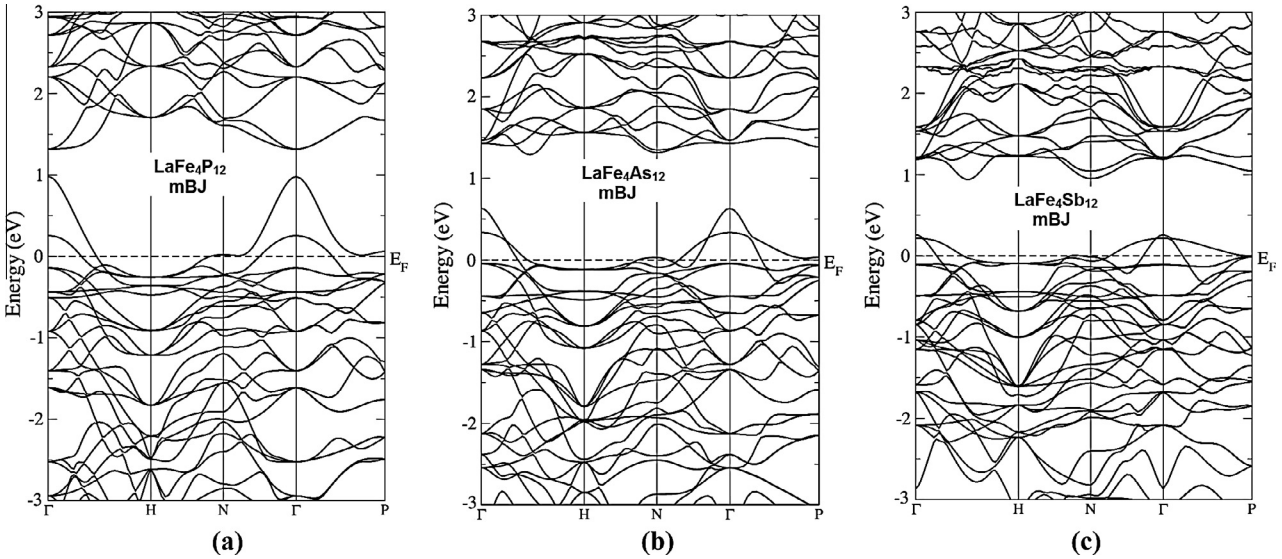

Fig. 2. Calculated electronic band structure of $LaFe_4X_{12}$ (X = P, As and Sb) compounds using *mBJ* approach.

the investigated compound. The *FPLAPW + lo* method has proven to be one of the accurate methods for the computation of the electronic structure of solids within density functional theory (*DFT*) [29–33].

2. Details of calculations

This work is devoted to study some specific features of the electronic structure of skutterudites $LaFe_4X_{12}$ (X = P, As and Sb) compounds. These compounds crystallizes in cubic space group Im−3. In the unit cell, La atom is situated at (0.0, 0.0, 0.0), Fe at (0.25, 0.25, 0.25) and X at (0.0, *u*, *v*) [18,19]. Fig. 1(a–c) illustrates the crystal structure of $LaFe_4X_{12}$ (X = P, As and Sb). The lattice constant *a* and the two internal free parameters *u* and *v* were optimized by minimizing the total energy. The optimization is achieved using the full potential linear augmented plane wave (*FPLAPW + lo*) method as implemented in WIEN2k code [34] within the local density approximation (*LDA*) [35]. These values are listed in Table 1 along with the with the bulk modulus *B* in (GPa) and its pressure derivative, *B′* in comparison with the experimental data and the previous results [19,20,22,36–38]. The experimental atomic positions [18,19] were optimized by minimizing the forces acting on each atom, we assume that the structure is totally relaxed when the forces on each atom reach values less than 1 mRy/a.u. The optimization of the atomic position were achieved using Perdew, Burke and Ernzerhof generalized gradient approximation (*PBE-GGA*) [39]. From the obtained relaxed geometry the electronic structure, the chemical bonding, electronic charge density and the optical properties have been determined using *FPLAPW + lo* within the recently modified Becke–Johnson potential (*mBJ*). To solve the Kohn–Sham equations a basis of linear APW's were used. In the muffin-tin (*MT*) spheres the potential and charge density were expanded in spherical harmonics with $l_{max} = 8$ and nonspherical components up to $l_{max} = 6$. In the interstitial region the potential and the charge density were represented by Fourier series. Self-consistency was obtained using 800 $\vec{k}$ points in the irreducible Brillouin zone (*IBZ*). The electronic band structure and the related properties were calculated within 5000 $\vec{k}$ points in *IBZ*. The self-consistent calculations were converged since the total energy of the system was stable within 10^{-5} Ry.

3. Results and discussion

3.1. Electronic band structure and density of states

The calculated electronic band structure of $LaFe_4X_{12}$ (X = P, As and Sb) compounds within *mBJ* are plotted in Fig. 2(a)–(c) along the high symmetry directions $\Gamma \rightarrow H \rightarrow N \rightarrow \Gamma \rightarrow P$ of the FCC cubic structure. The Fermi level is situated at 0.0 eV. It is clear that moving from P → As → Sb show significant influence on the bands dispersion, for instance the bands below Fermi level which are mainly consist of Fe-d and X-p states shifts toward Fermi level. It has been noticed that for the investigated compounds only two bands cuts Fermi level to form Fermi surface. To the best of our knowledge no experimental data on the electronic band structure of $LaFe_4X_{12}$ (X = P, As and Sb) compounds have appeared in the literature to make a meaningful comparison. Therefore, we can compare our calculated electronic band structure with previous calculations using different methods and different exchange–correlation potentials [20–23], in general reasonable agreement was found in the matter of bands dispersion. Based on our previous experiences with *mBJ* on similar systems [40,41] therefore, using *mBJ* to calculate the electronic band structure of $LaFe_4X_{12}$ (X = P, As and Sb) compounds should show better band splitting than that obtained from *LDA* and *GGA* and hence more accurate optical properties due to better optical transitions between the bands. Future experimental work will testify our calculated results. In order to inspect the influence of substituting P → As → Sb on the bands/states dispersions, bond lengths and angles, the hybridization between the orbitals and the types of orbitals which are control the overlapping around Fermi level, we investigated the total and the angular momentum resolved projected density of states (*TDOS* and) *PDOS* using *mBJ* approach as illustrated in Figs. 3(a)–(j). Fig. 3(a) presents the influence of substituting P → As → Sb on the *TDOS* which confirm that there is significant influence on the bands dispersion. The calculated partial density of states are presented in Fig. 3(b)–(j) which explore that the Fe-d state has the main contribution around Fermi level along with small contribution from Fe-s/p and X-s/p states. These states control the overlapping around Fermi level, the overlapping is strong enough indicating the metallic nature of the investigated compound with increasing value of the density of states at Fermi level $N(E_F)$ when

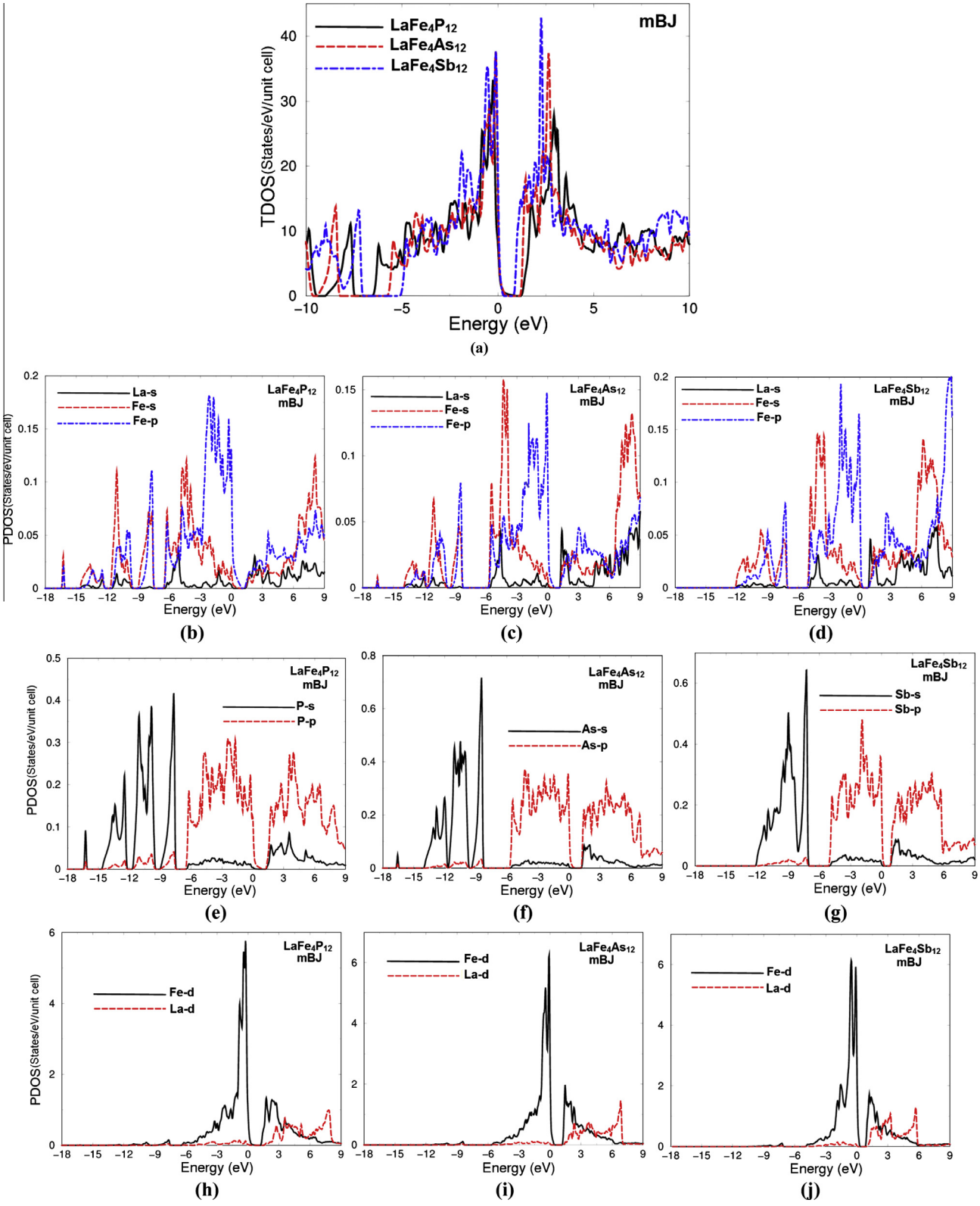

Fig. 3. Calculated total and partial density of states of $LaFe_4X_{12}$ (X = P, As and Sb) compounds using *mBJ* approach.

we move from P → As → Sb. The associated electronic specific heat coefficient (γ) can be determined by using the expression, $\gamma = \frac{1}{3}\pi^2 N(E_F)k_B^2$ where k_B is the Boltzmann constant. The calculated values of $N(E_F)$ and γ for $LaFe_4X_{12}$ (X = P, As and Sb) compounds are listed in Table 2. It is clear that these values are increases with substituting P → As → Sb that is attributed to the fact that just below Fermi level (E_F) there exists several bands with less dispersion moves close to E_F when we substitute P → As → Sb. Also due to the fact that the atomic radii of Sb (145 pm) > As (115 pm) > P (100 pm), this lead to increase the bond lengths between the atoms which cause to push up electronic energy on the neighboring atoms resulting in increasing $N(E_F)$ and hence γ. It is interesting

Table 2
Calculated density of states at Fermi lever N(E_F) for $LaFe_4X_{12}$ (X = P, As and Sb) along with the calculated electronic specific heat coefficient (γ).

Compound	N(E_F)	γ
$LaFe_4P_{12}$	17.20 (states/Ry/cell) 190 (states/Ry) [a]	2.98 (mJ/mole K^2)
$LaFe_4As_{12}$	27.40 (states/Ry/cell) 247 (states/Ry) [a]	4.75 (mJ/mole K^2)
$LaFe_4Sb_{12}$	44.51(states/Ry/cell) 343 (states/Ry) [a]	7.71 (mJ/mole K^2)

[a] Ref. [20].

to mention that due to the small electro-negativity differences between P (2.19), As (2.18) and Sb (2.05) therefore, substituting P → As → Sb will not introduce more peaks in the density of states [42]. The calculated angular momentum resolved projected density of states enables us to identify the angular momentum characters of the various structures. It has been found that La-s, Fe-s/p and X-s/p states are contributing along the whole energy range. While the contribution of Fe-d state is confined in two regions (−6.0 up to 0.5) eV and (0.1 and above), the contribution of La-d start from 1.5 eV.

There exists a strong hybridization between Fe-s and Fe-p states, whereas a weak hybridization is found between Fe-s, Fe-p and La-s states and X-s strongly hybridized with X-p state therefore, most the bonds have ionic nature except the X atoms are forming strong covalent bonds. To investigate the bonds nature and the interactions between the atoms we have taken a deep careful look at valence band electronic charge density distribution of $LaFe_4X_{12}$ (X = P, As and Sb) compounds in two crystallographic planes namely (100) and (101) as shown in Fig. 4(a)–(f). It has been observed that the (100) plane exhibit only La and X atoms, La atoms surrounding by spherical charge indicating the ionic nature of these atoms while the X atoms form strong covalent bonding with the neighboring X atoms. Whereas the (101) plane exhibit all the atoms where Fe atoms surrounding by uniform spherical charge indicating the ionic nature. Due to electronegativity differences between La (1.1), Fe (1.83), P (2.19), As (2.18) and Sb (2.05) one can see that the charge is attracted toward X atoms which is clearly shown by the blue[1] (1.0000) color which is corresponds to the maximum charge accumulation site according to charge density scale.

It has been mentioned earlier the calculated electronic band structure of $LaFe_4X_{12}$ (X = P, As and Sb) compounds exhibit that only two bands crossing Fermi level to form Fermi surface in concordance with our observation from the partial density of states at Fermi level. These bands are mainly consist of Fe-d states and X-p states. The Fermi level is determined via the Kohn–Sham eigenvalue of the highest occupied state. The shape of Fermi surface is shown in Fig. 5(a)–(c). The observed Fermi surface consists of empty areas that represent the holes and shaded areas corresponding to the electrons.

3.2. Optical properties

The complex dielectric function $\varepsilon(\omega)$ is well explained the optical properties of materials, which represents the linear response of a system to an external electromagnetic field. It can be expressed as $\varepsilon(\omega) = \varepsilon_1(\omega) + i\varepsilon_2(\omega)$, where $\varepsilon_1(\omega)$ and $\varepsilon_2(\omega)$ are the real and imaginary parts of the dielectric function. The imaginary part $\varepsilon_2(\omega)$ is directly related to the electronic band structure of the material and describes its absorptive behavior [43]. This quantity can be computed by summing up all possible transitions from the occupied to the unoccupied states, taking into account the appropriate transition dipole matrix elements. The real part $\varepsilon_1(\omega)$ can be derived from the imaginary part using Kramers–Kronig transformation [43]. The calculations of the optical dielectric function involve the energy eigenvalues and electron wave functions which are natural outputs of band structure calculations. The knowledge of both real and imaginary parts of the dielectric function allows the calculation of various optical constants, such us the reflectivity spectra, $R(\omega)$ refractive index, $n(\omega)$ loss function $L(\omega)$ and absorption coefficient $I(\omega)$. $LaFe_4X_{12}$ (X = P, As and Sb) compounds have face-centred cubic structure with space group Im−3. For calculating the optical properties of cubic structural material only one dielectric tensor component we need to completely characterize the linear optical properties. This component is $\varepsilon_2(\omega)$ the imaginary part of the frequency dependent dielectric function is given by Ref. [44]

$$\varepsilon_2(\omega) = \frac{8}{3\pi\omega^2}\sum_{nn'}\int_{BZ}|P_{nn'}(k)|^2\frac{dS_k}{\nabla\omega_{nn'}(k)} \quad (1)$$

where $P_{nn'}$ is the dipolar matrix elements between initial $|nk\rangle$ and final $|n'k\rangle$ states with their eigenvalues $E_n(k)$ and, $E_{n'}$, respectively. For the metallic and semimetallic materials there are two contribution to, $\varepsilon_2(\omega)$ namely intra-band and inter-band transitions. As the investigated compounds are metallic we must include the Drude term (intraband transitions) [43].

$$\varepsilon_2(\omega) = \varepsilon_{2\text{inter}}(\omega) + \varepsilon_{2\text{intra}}(\omega) \quad (2)$$

where

$$\varepsilon_{2\text{intra}}(\omega) = \frac{\omega_P\tau}{\omega(1+\omega^2\tau^2)} \quad (3)$$

where ω_P is the anisotropic plasma frequency [43] and τ is the mean free time between collisions.

$$\omega_P^2 = \frac{8\pi}{3}\sum_{kn}\vartheta_{kn}^2\delta(\varepsilon_{kn}) \quad (4)$$

where ε_{kn} is $E_n(k) - E_F$ and ϑ_{kn} is the electron velocity. In Table 3, we have listed the values of the plasma frequency for the investigated compounds.

To ascertain the effect of intra-band transitions on the optical dielectric functions, we have calculated $\varepsilon_2(\omega)$ and $\varepsilon_1(\omega)$ with and without inclusion of the Drude term. In Fig. 6(a) and (b) we illustrated $\varepsilon_2(\omega)$ and $\varepsilon_1(\omega)$ with Drude term. It has been found that the intra-band transitions have significant effect at energies ⩽1.0 eV. The sharp rise below 1.0 eV is due to the intra-band transitions. A lossless region appears around 1.2 eV. The dispersion of the imaginary part of the optical dielectric function for $LaFe_4X_{12}$ (X = P, As and Sb) compounds show that substituting P → As → Sb lead to shift the spectral structure toward lower energies with increasing the amplitude. This observation could be

[1] For interpretation of color in Figs. 4, the reader is referred to the web version of this article.

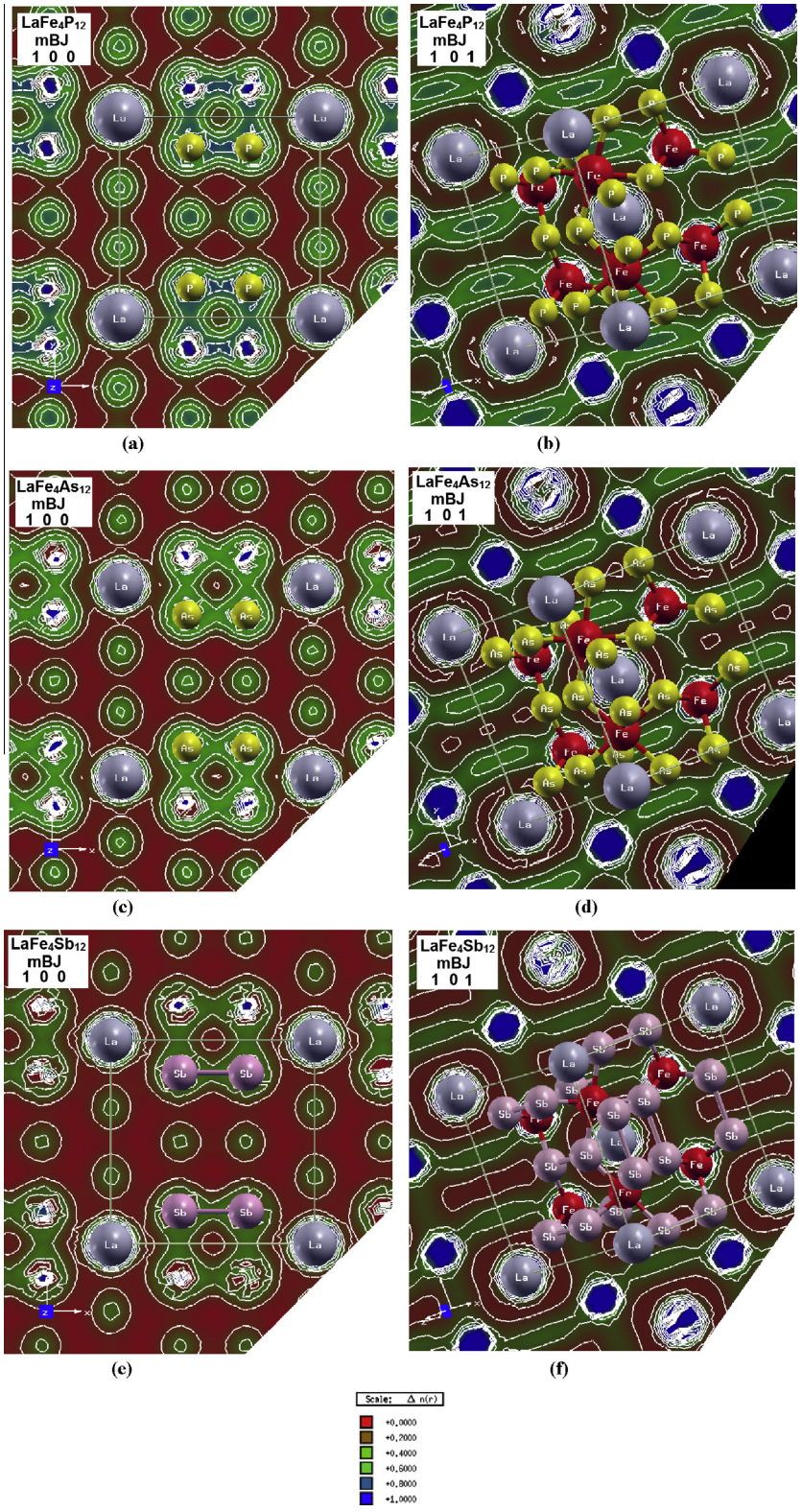

Fig. 4. Calculated electronic charge density dispersion of $LaFe_4X_{12}$ (X = P, As and Sb) compounds using *mBJ* approach for two crystallographic planes (1 0 0) and (1 0 1).

attributed to increasing of the bond lengths while we replacing P → As → Sb due to the increasing/reducing the atomic radii P (100 pm) < As (115 pm) < Sb (145 pm). In all cases the optical spectral structure of the imaginary part present only one main peak. We make use of the calculated electronic band structure and partial density of states with aid of the optical selection rules and the optical matrix elements to analyze the optical transitions that are responsible for the spectral features in $\varepsilon_2(\omega)$. It has been found that the observed spectral structures are correspond to the electric–dipole transitions that have large optical matrix elements. The real part of the optical dielectric function are shown in Fig. 6(b). It confirms that the intra-band transitions have

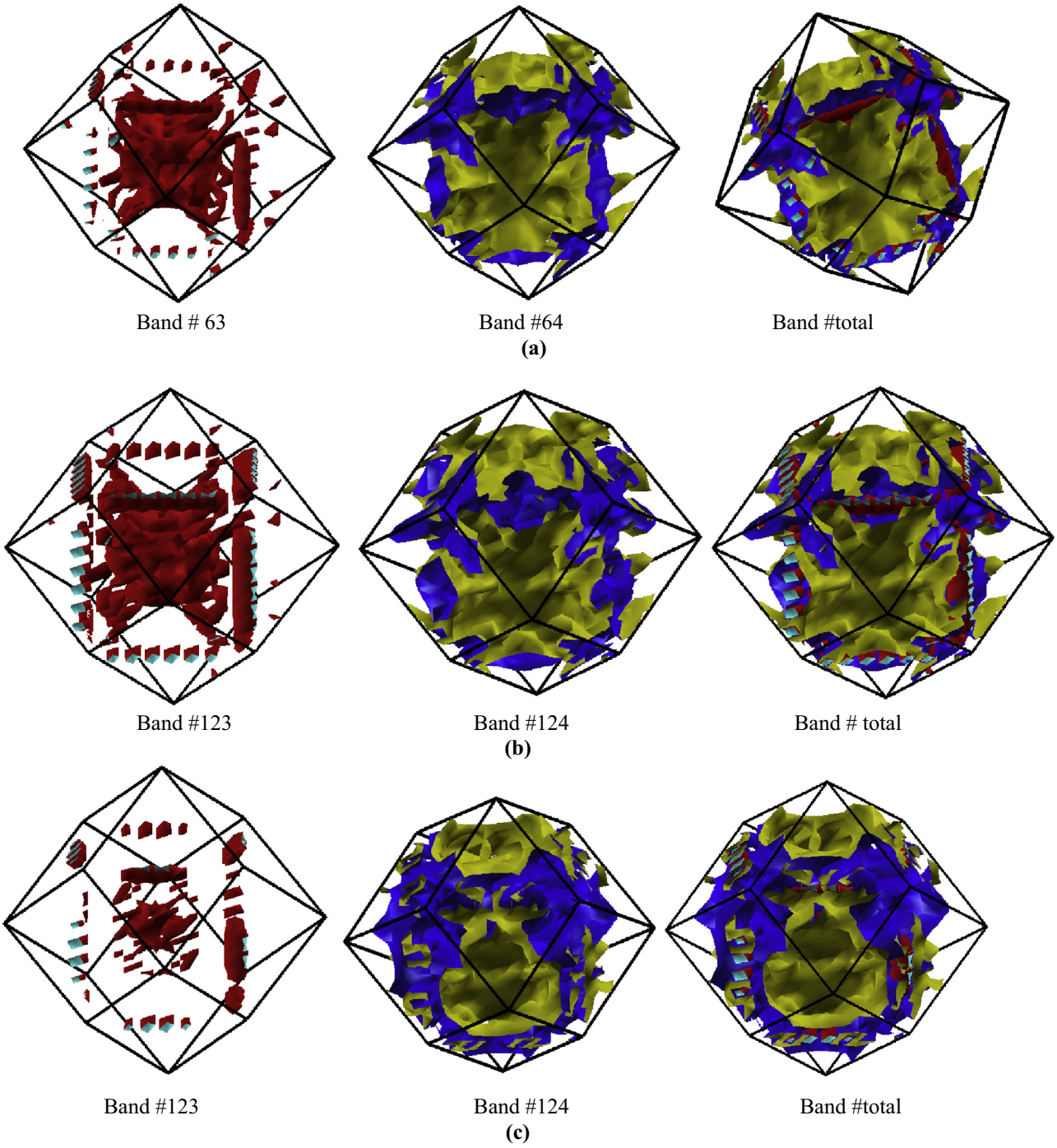

Fig. 5. Calculated Fermi surface of $LaFe_4X_{12}$ (X = P, As and Sb) compounds using *mBJ* approach.

significant effect at energies $\leqslant$1.0 eV, and the spectral structure shift toward lower energies when we replace P by As and As by Sb.

The calculated reflectivity spectra of $LaFe_4X_{12}$ (X = P, As and Sb) compounds are illustrated in Fig. 6(c). We observe that a high reflectivity ($\sim$unity) occurs at low energies followed by a lossless region around 1.2 eV. The first reflectivity minima occurs at 9.0 eV. The reflectivity minima confirm the occurrence of a collective plasmon resonance. The depth of the plasmon minimum is determined by the imaginary part of the dielectric function at the plasma resonance and is representative of the degree of overlap between the inter-band absorption regions. Fig. 6(d) illustrated the calculated absorption coefficient which explore that $LaFe_4X_{12}$ (X = P, As and Sb) compounds have zero absorption at low energy ($\leqslant$1.0 eV) confirming that this compound possesses high reflectivity ($\sim$unity), thereafter the absorption increases rapidly with increasing the energy of the incident photons. The calculated

Table 3
The calculated, ω_p^{xx} ω_p^{yy} and ω_p^{zz} $LaFe_4X_{12}$ (X = P, As and Sb) when, $\varepsilon_1^{xx}(\omega)$ $\varepsilon_1^{yy}(\omega)$ and $\varepsilon_1^{zz}(\omega)$ cross zero.

Compound	ω_p^{xx}
$LaFe_4P_{12}$	1.596
$LaFe_4As_{12}$	1.765
$LaFe_4Sb_{12}$	1.951

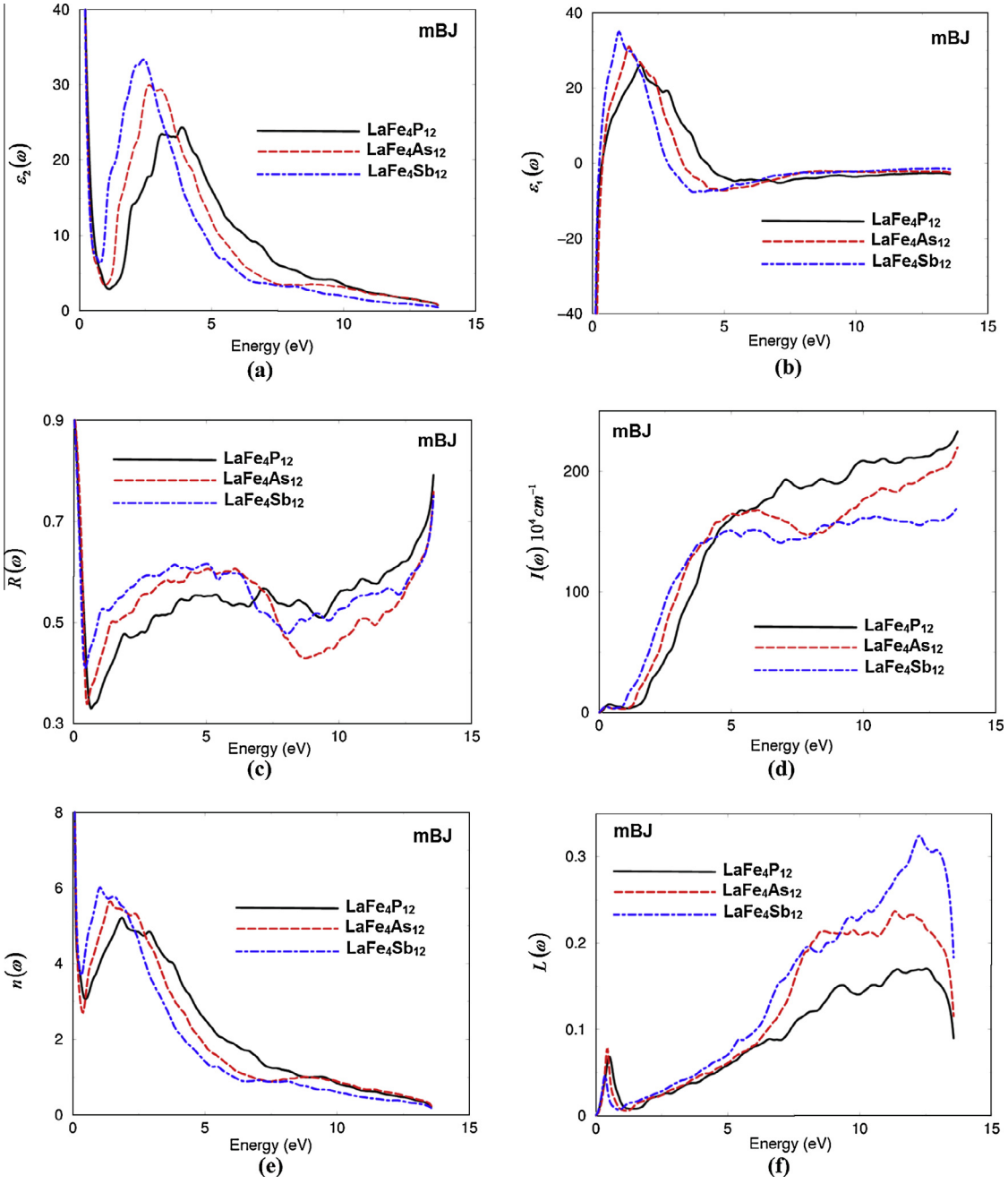

Fig. 6. Calculated optical properties of $LaFe_4X_{12}$ (X = P, As and Sb) compounds using *mBJ* approach; (a) imaginary part; (b) real part; (c) reflectivity spectra; (d) absorption coefficient; (e) refractive indices; (f) loss function.

refractive indices $n(\omega)$ as represented in Fig. 6(e) exhibit high values of the refractive indices at low energies and thereafter drop to low values (lossless region) then it forms the main peak at around 1.5, 2.0 and 2.5 eV for $LaFe_4X_{12}$ (X = P, As and Sb), respectively. Again it show that the spectral structure shift toward lower energies when we replace P by As and As by Sb. Fig. 6(f) illustrated the loss function, there exists two lossless regions, low lossless region at around 1.0 eV and the high lossless region at around 12.5 eV in concordance with our previous observation from Fig. 6(a)–(e).

4. Conclusions

The all-electron full potential linear augmented plane wave plus local orbitals (*FPLAPW + lo*) method within the recently modified Becke–Johnson potential were employed to investigated some specific features of $LaFe_4X_{12}$ (X = P, As and Sb) compounds. The lattice constant a and the two internal free parameters u and v were optimized by minimizing the total energy. The optimization is achieved using *LDA*. The results show good agreement with the experimental data and the previous theoretical results. The experimental atomic positions were optimized by minimizing the forces acting on each atom, we assume that the structure is totally relaxed when the forces on each atom reach values less than 1 mRy/a.u. The optimization of the atomic position were achieved using *PBE-GGA*. The calculated electronic band structure and density of states explore that there is a significant influence on the bands/states dispersions when we substituting P → As → Sb. The values of $N(E_F)$ and γ confirm the increasing in the metallicity of the investigated materials when we move P → As → Sb. The partial density of states show there exists a strong hybridization between

Fe-s and Fe-p states, whereas a weak hybridization is found between Fe-s, Fe-p and La-s states and X-s strongly hybridized with X-p state therefore, most the bonds have ionic nature except the X atoms are forming strong covalent bonds. This observation was confirmed by the calculated electronic charge density distribution. Fermi surface was calculated and it has been found that it is consists of empty areas that represent the holes and shaded areas corresponding to the electrons. To get deep insight into the electronic structure, the optical properties were calculated which show that when we replace P by As and As by Sb the spectral structure shift toward lower energies in concordance with our observation from the electronic band structures and the density of states. Also it shows there exists a lossless regions.

Acknowledgments

The result was developed within the CENTEM project, Reg. No. CZ.1.05/2.1.00/03.0088, cofunded by the ERDF as part of the Ministry of Education, Youth and Sports OP RDI programme and, in the follow-up sustainability stage, supported through CENTEM PLUS (LO1402) by financial means from the Ministry of Education, Youth and Sports under the "National Sustainability Programme I. Computational resources were provided by MetaCentrum (LM2010005) and CERIT-SC (CZ.1.05/3.2.00/08.0144) infrastructures.

References

[1] G.D. Mahan, H. Ehreinreich, F. Spaepen (Eds.), Solid State Physics, vol. 51, Academic Press, New York, 1998. 81.
[2] B.C. Sales, D. Madrus, B.C. Chakoumakos, V. Keppens, J.R. Thompson, Phys. Rev. B 56 (1997) 15081.
[3] G.S. Nolas, J.L. Cohn, G.A. Slack, Phys. Rev. B 58 (1998) 164.
[4] G.P. Meisner, M.S. Torikachvili, K.N. Yang, M.B. Maple, R.P. Guertin, J. Appl. Phys. 57 (1985) 3073.
[5] I. Shirotani, T. Uchiumi, C. Sekine, S. Kimura, N. Hamaya, J. Solid State Chem. 142 (1999) 146.
[6] I. Shirotani, T. Uchiumi, K. Ohno, C. Sekine, Y. Nakazawa, K. Kanoda, S. Todo, T. Yagi, Phys. Rev. B 56 (1997) 7866.
[7] T. Uchiumi, I. Shirotani, C. Sekine, S. Todo, T. Yagi, Y. Nakazawa, K. Kanoda, J. Phys. Chem. Solids 60 (1999) 689.
[8] E.D. Bauer, N.A. Frederick, P.-C. Ho, V.S. Zapf, M.B. Maple, Phys. Rev. B 65 (2002) 100506R.
[9] M.S. Torikachvili, C. Rossel, M.W. McElfresh, M.B. Maple, R.P. Guertin, G.P. Meisner, J. Magn. Magn. Mater. 54 (1986) 365.
[10] M.E. Danebrock, C.B.H. Evers, W. Jeitschko, J. Phys. Chem. Solids 57 (1996) 381.
[11] L. Keller, P. Fischer, T. Herrmannsdörfer, A. Dönni, H. Sugawara, T.D. Matsuda, K. Abe, Y. Aoki, H. Sato, J. Alloys Compd. 323 (2001) 516.
[12] K. Tenya, N. Oeschler, P. Gegenwart, F. Steglich, N.A. Frederick, E.D. Bauer, M.B. Maple, Acta Phys. Pol., B 34 (2003) 995.
[13] C. Sekine, T. Uchiumi, I. Shirotani, K. Matsuhira, T. Sakakibara, T. Goto, T. Yagi, Phys. Rev. B 62 (2000) 11581.
[14] C. Sekine, T. Uchiumi, I. Shirotani, T. Yagi, Phys. Rev. Lett. 79 (1997) 3218.
[15] S.V. Dordevic, D.N. Basov, N.R. Dilley, E.D. Bauer, M.B. Maple, Phys. Rev. Lett. 86 (2001) 684.
[16] A. Yamasaki, S. Imada, T. Masuda, T. Nanba, A. Sekiyama, H. Sugawara, T.D. Matsuda, H. Sato, C. Sekine, I. Shirotani, H. Harima, S. Suga, Acta Phys. Pol., B 34 (2003) 1035.
[17] E.D. Bauer, A. Slebarski, E.J. Freeman, C. Sirvent, M.B. Maple, J. Phys.: Condens. Matter 13 (2001) 4495.
[18] F. Grandjean, A. Gérard, D.J. Braun, W. Jeitschko, J. Phys. Chem. Solids 45 (1984) 877.
[19] W. Jeitschko, D.J. Braun, Acta Crystallogr. 33 (1977) 3401.
[20] Hisatomo Harima, Katsuhiko Takegahara, Physica B 328 (2003) 26–28.
[21] Katsuhiko Takegahara, Hisatomo Harima, J. Magn. Magn. Mater. 310 (2007) 861–863.
[22] M. Hachemaoui, R. Khenata, A. Bouhemadou, S. Bin-Omran, Ali H. Reshak, F. Semari, D. Rached, Solid State Commun. 150 (2010) 1869–1873.
[23] K. Nouneh, Ali H. Reshak, S. Auluck, I.V. Kityk, R. Viennois, S. Benet, S. Charar, J. Alloys Compd. 437 (2007) 39–46.
[24] K. Nouneh, R. Viennois, I.V. Kityk, F. Terki, S. Charar, S. Benet, S. Paschen, Phys. State Solid (b) 241 (13) (2004) 3069–3080.
[25] M.I. Kolinko, I.V. Kityk, A.S. Krochuk, J. Phys. Chem. Solid 53 (10) (1992) 1315–1320.
[26] M. Matusiewicz, M. Czerwinski, J. Kasperczyk, I.V. Kityk, J. Chem. Phys. 111 (14) (1999) 6446–6455.
[27] A.H. Reshak, M. Piasecki, S. Auluck, I.V. Kityk, R. Khenata, B. Andriyevsky, C. Cobet, N. Esser, A. Majchrowski, O.M. Swirkowicz, R. Diduszko, W. Szyrski, J. Phys. Chem. B 113 (2009) 15237–15242.
[28] F. Tran, P. Blaha, Phys. Rev. Lett. 102 (2009) 226401.
[29] A.H. Reshak, S. Azam, Opt. Mater. 37 (2014) 97–103.
[30] A.H. Reshak, S. Auluck, Opt. Mater. 38 (2014) 80–86.
[31] A.H. Reshak, S.A. Khan, Z.A. Alahmed, Opt. Mater. 37 (2014) 322–326.
[32] A.H. Reshak, Opt. Mater. http://dx.doi.org/10.1016/j.optmat.2015.04.022.
[33] Hardev S. Saini, Mukhtiyar Singh, A.H. Reshak, Manish K. Kashyap, J. Magn. Magn. Mater. 331 (2013) 1–6.
[34] P. Blaha, K. Schwarz, G.K.H. Madsen, D. Kvasnicka, J. Luitz, WIEN2k, An Augmented Plane Wave Plus Local Orbitals Program for Calculating Crystal Properties, Vienna University of Technology, Austria, 2001.
[35] J.P. Perdew, A. Zunger, Phys. Rev. B 23 (1981) 5048.
[36] T. Kamagai, Y. Nakanishi, H. Sugawara, H. Sato, M. Yoshizawa, Physica B 329 (2003) 471.
[37] Y. Nakanishi, T.D. Matsuda, H. Sugawara, H. Sato, M. Yoshizawa, Physica B 312 (2002) 827.
[38] C. Recknagel, N. Reinfried, P. HÖhn, W. Schnelle, H. Rosner, Yu. Grin, A. Leithe-Jasper, Sci. Technol. Adv. Mater. 8 (2007) 357.
[39] J.P. Perdew, S. Burke, M. Ernzerhof, Phys. Rev. Lett. 77 (1977) 3865.
[40] A.H. Reshak, RSC Adv. 5 (2015) 33632.
[41] A.H. Reshak, RSC Adv. 4 (2014) 64947.
[42] Joo-Hyoung Lee, Junqiao Wu, Jeffrey C. Grossman, Phys. Rev. Lett. 104 (2010) 016602.
[43] F. Wooten, Optical Properties of Solids, Academic press, New York, USA, 1972.
[44] M.A. Khan, Arti Kashyap, A.K. Solanki, T. Nautiyal, S. Auluck, Phys. Rev. B 23 (1993) 16974.